AIAA 2002-2524

Noise Control Using Adjoint-based Optimization

M. Wei and J. B. Freund
Theoretical and Applied Mechanics
University of Illinois at Urbana-Champaign
Urbana, Illinois 61801

8th AIAA/CEAS Aeroacoustics Conference
June 17–19, 2002/Breckenridge, CO

Noise Control Using Adjoint-based Optimization

M. Wei* and J. B. Freund†
Theoretical and Applied Mechanics
University of Illinois at Urbana-Champaign
Urbana, Illinois 61801

Attempts to control the jet noise have been hampered by an insufficent understanding of its mechanisms, resulting in a reliance on trial-and-error experimentation to reduce noise. This paper aims to explore the noise mechanism using adjoint-based noise control in conjunction with a direct numerical simulation. A control problem is formulated with the objective of reducing acoustic intensity on a line in the sound field. The cost function that quantifies this is used to force the adjoint of the compressible flow equation, which are solved numerically in the same way we solve the flow equations. The adjoint variables provide the sensitivity of the noise, as we have specifically defined it, to changes in actuation. Using this approach, the noise radiated from a two-dimensional mixing layer with convective Mach number $M_c = 0.4$ and Reynolds number based on vorticity thickness $Re_\omega = 500$ was reduced by 6.3dB. This flow is a model of the near nozzle region of a jet and generalization of the technique to a jet is straightforward. Despite the substantial reduction in the noise, the changes of the flow field are small, as seen by examination of the turbulence kinetic energy and the momemtum thickness before and after control is applied. We conclude that the controler makes subtle changes to the radiating portion of the flow without drastically altering its energetics. Our preliminary investigations into the nature of the automatically identified control reveal little of how it works.

Nomenclature

a	Sound speed
$\mathcal{C}$	Control region
f	Frequency
f_0	Fundamental frequency
F_e	Excitation forcing
$\mathbf{g}$	Gradient for control update
k	Turbulent kinetic energy (TKE)
K	Integrated quantity of TKE
M	Mach number
M_c	Convective Mach number $= \frac{U_1+U_2}{2a_\infty}$
p	Pressure
Re_ω	Reynolds number $= \frac{\rho\delta_\omega\Delta U}{\mu}$
St	Strouhal number $= \frac{f\delta_m}{U_c}$
t	Time
Δt	Timestep
u, v	Velocity in x and y
U_1	Speed of high-speed stream (top)
U_2	Speed of low-speed stream (bottom)
U_c	Approximate convection speed $= \frac{U_1+U_2}{2}$
ΔU	$U_1 - U_2$
x, y	Cartesian coordinates
α	Line search parameter for control update
β	Initial phases of excitation
δ_m	Momentum thickness
δ_ω	Vorticity thickness
μ	Viscosity
ρ	Density
ϕ	Control
ψ	Excitation function
Ω	Noise reduction line (target line)

Accents/Subscripts/Superscripts

$\overline{()}$	Time average
∞	Ambient
$'$	Perturbation from mean
n	Iteration #
$*$	Adjoint variable

Introduction

JET noise remains a significant component of aircraft noise, and thus, as noise regulations become more restrictive, it will affect the attractiveness of planes and engines on the market. Although theoretical noises were first formulated 50 years ago,[1] their direct use in modeling and control has been hampered by the lack of a detailed quantitative description of the flow field. Even with this information, provided recently for the first time by direct numerical simulation (DNS),[2–5] effective controls are not obvious due to the complexity of the flow.

It has been known for a long time that certain nozzle geometry modifications reduce noise. Lobes[6] can quiet the exhaust, but cause unacceptable thrust loss. So-called hush kits are retrofit to engines to mix the flow internally to reduce noise outside, but again with significant losses. Recently, chevrons (triangles cut out of the nozzle lip essentially parallel to the flow) have been found to reduce noise a couple decibels (effective perceived noise) with minimal incurred loss.[7,8] However, since trial-and-error experimentation is a component of

*Research Assistant.

†Assistant Professor. AIAA member.

their design, there is no way of knowing how effective they can ultimately be. Active control can in principle offer greater control authority by its nature, but it is simply not known how to use available actuators or how to optimize actuator designs to reduce noise. Understanding of jet noise is too limited (or jet noise is too complex) to provide effective models, even at a phenomenological level, that can be used in an optimization procedure.

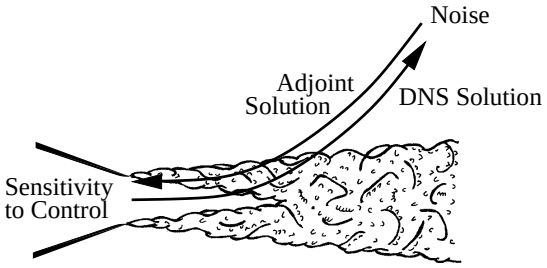

Fig. 1 Schematic of the adjoint-based procedure for determining control sensitivity.

Our approach is an automatic control optimization that employs the adjoint of the compressible flow equation, as previewed in authors' previous work.[9] It circumvents our poor understanding of the mechanisms and provides automatic means of reducing noise despite its complexity. The approach is shown schematically in figure 1. Given a numerical solution of the compressible flow equations for a jet, which currently can only be provided by an accurate flow simulation, the adjoint of these equations is solved numerically backward in time to give the sensitivity of the noise, as defined quantitatively by an appropriate metric, to changes in the control at the nozzle. This sensitivity is used to update controls for the specific noise reduction objective that we have selected. As formulated, success depends upon the full flow field information of a DNS, so it is obviously not directly practical. Our intention is to develop general laws and guide future experiments and designs and to achieve a better understanding of what is currently a poorly understood mechanism. Several avenues of generalization are being pursued, but are not discussed in this paper.

The Two-dimensional Mixing Layer

We demonstrate the algorithm and study its results when it is applied to the two-dimensional mixing layer shown in figure 2. The Reynolds number is $Re_\omega = 500$, based on vorticity thickness,

$$\delta_\omega = \left(\frac{\Delta U}{|du/dy|_{max}} \right)_{x=0}, \tag{1}$$

the Mach numbers of the top and bottom streams are $M = 0.8$ and $M = 0.0$, respectively. The inflow temperature is uniform.

The black line Ω in figure 2 at $y = -40\delta_\omega$ and extending between $x = 10\delta_\omega$ and $x = 40\delta_\omega$ is our *target line*, where the noise will be reduced. The actuation is a generic forcing term $\phi(\mathbf{x},t)$ added to the right-hand-side of the energy equation in a small control region $\mathcal{C}$, $x/\delta_\omega \in (1,5)$ and $y/\delta_\omega \in (-2,2)$, also shown in the figure.

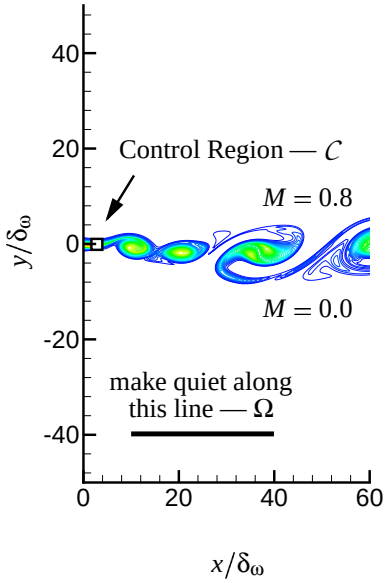

Fig. 2 Mixing layer control schematic.

Control Formulation

Our control objective is to reduce the cost functional

$$\mathcal{J}(\phi) = \int_{t_0}^{t_1} \int_\Omega (p - p_\infty)^2 \, d\Omega \, dt, \tag{2}$$

where p is the instantaneous pressure, p_∞ is the ambient pressure, and t_0 and t_1 are the beginning and end of the times to be made quiet. To determine the sensitivity of $\mathcal{J}$ to small modifications of the control ϕ, we consider a $\mathcal{J}'$ perturbation to the cost $\mathcal{J}$ resulting from a perturbation ϕ' to the control ϕ.[10] $\mathcal{J}'$ is the Fréchet differential of the cost functional $\mathcal{J}$:

$$\begin{aligned} \mathcal{J}'(\phi;\phi') &\equiv \frac{\mathcal{D}\mathcal{J}(\phi)}{\mathcal{D}\phi} \cdot \phi' \\ &\equiv \lim_{\varepsilon \to 0} \frac{\mathcal{J}(\phi + \varepsilon\phi') - \mathcal{J}(\phi)}{\varepsilon} \\ &= \int_{t_0}^{t_1} \int_\Omega 2pp' \, d\Omega dt. \end{aligned} \tag{3}$$

This form of $\mathcal{J}'$ provides the gradient direction $\mathbf{g}$, in which to adjust ϕ to reduce $\mathcal{J}$. Instead of being solved directly via (3) as expressed in the physical flow variables, the gradient $\mathbf{g}$ is more easily determined from a solution of the adjoint system,[9] as forced by $\mathcal{J}$, using a well-documented procedure.[10]

Then, the control is updated as

$$\phi^{n+1} = \phi^n - \alpha^n \mathbf{g}^n, \tag{4}$$

where α^n is a line-search parameter determining the change along direction $\mathbf{g}^n$ for the n^{th} iteration. The Polak-Ribiere variant of the conjugate gradient algorithm is used with Brent's line-minimization method[11] to accelerate convergence.

There are 920 mesh points in the control region $\mathcal{C}$ and we attempt to reduce the noise for $t_1 - t_0 = 200\delta_\omega/a_\infty$. ϕ is free to assume any value at any of the space time points. Given out timestep $\Delta t = 0.05\delta_\omega/a_\infty$, we are optimizing 3.84×10^6 free parameters. Direct exploration of this parameter space is clearly prohibitive.

Computational Methods

The flow and sound fields are governed by the compressible Navier-Stokes equations, which are solved numerically in two space dimensions without modeling assumptions using a fourth-order Runge-Kutta algorithm for time advancement. For spatial differencing, a sixth-order Padé scheme[12] is used in the x (streamwise) direction, and the Dispersion-Relation-Preserving (DRP) scheme[13] is used in the y (cross-stream) direction. The explicit DRP scheme facilitates decomposition across different processor on a parallel machine. A specialized buffer zone similar to that of Freund[14] and a more traditional non-reflecting boundary condition[15] are used in combination to absorb disturbances as they leave the finite computational domain. The same schemes are used to solve the adjoint equations, also without modeling approximations.

Instability theory predicts that the most unstable mode of the incompressible mixing layer to have $St = 0.032$,[16,17] which provides an estimation of the fundamental frequency of our compressible mixing layer, since this frequency is not very sensitive to compressibility for $M_c = 0.4$.[18,19] So we take our fundamental frequency to be $f_0 = \frac{St\,U_c}{\delta_m}$. Numerical experimentation confirms that the mixing layer does respond strongly to forcing at or near this frequency. To provide a richer flow for our scheme to control, we excite the flow at a total of eight frequencies, $f_0/4$, $f_0/2$, $3f_0/4$, f_0, $5f_0/4$, $3f_0/2$, $7f_0/4$, and $2f_0$. These were selected in an *ad hoc* fashion in this study. A more thorough investigation of the effects of this excitation on the noise and its controllability is underway.

To minimize the direct effect of the excitation on the sound field, we define a function ψ with the 8 frequencies f_i listed above, as

$$\begin{aligned}\psi = &\psi_0\, e^{-\sigma_x(x-x_0)^2} e^{-\sigma_y(y-y_0)^2} \\ &\times \sum_{i=1}^{8} \sin[2\pi f_i(x - x_0 - M_c t) + \beta_x^i] \\ &\times \sin[2\pi f_i(y - y_0) + \beta_y^i],\end{aligned} \tag{5}$$

where ψ_0 is the amplitude, (x_0, y_0) is $(-5\delta_\omega, 0)$, both σ_x and σ_y are 0.2, $\xi_{x,y}$ are initial random phases. The excitation, which appears as a bodyforce, is then defined as

$$F_{ex} = \frac{\partial \psi}{\partial y}, \quad F_{ey} = -\frac{\partial \psi}{\partial x}, \tag{6}$$

so that it is solenoidal and therefore relatively quiet. We observed no sound directly from this excitation. The amplitude of each mode was $\psi_0 = 0.004\rho_\infty a_\infty^2/\delta_\omega$. Our selection of x_0 and y_0 puts the excitation upstream of the physically realistic portion of the computation. Our controller, of course, has no direct knowledge of this excitation.

The flow was simulated for time $400\delta_\omega/a_\infty$ to allow it to reach a statistically stationary condition. Then the controller was turned on. We anticipate that the first $60\delta_\omega/a_\infty$ is uncontrollable based on the traveling time for the effect of the control to reach the target line Ω.

Noise Reduction

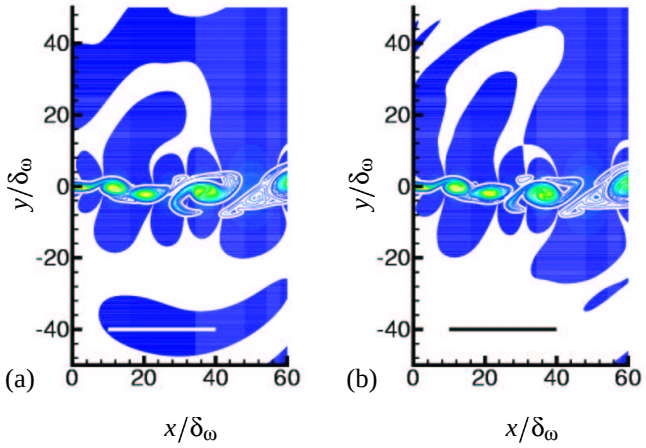

Fig. 3 Comparison of the flow and sound radiation (a) without control and (b) with control. Solid black is $|p'/p_\infty| > 0.003$. Contours show vorticity magnitude with peak $0.78a_\infty/\delta_\omega$.

Figure 3 (a) shows the instantaneous flow and sound field of the uncontrolled mixing layer with contours of vorticity to show the flow structure and regions of large $|p'|$ to mark acoustic radiation. The corresponding controlled case after 7 conjugate gradient iterations is shown in figure 3 (b) at the same time. The noise is clearly reduced along the target line.

This is confirmed quantitatively in figure 4, which shows a 77% reduction of cost functional, which is about 6.3dB. Furthermore, this sound reduction along the target line does not increase the noise elsewhere, as we showed before.[9] It is not anti-sound.

Adjoint Field

To better understand the control process, the evolution of the adjoint pressure p^* is shown in figure 5. It is this quantity that provides the gradient information g to update control equation (4). Since the flow equations are self-adjoint in the acoustic limit, the adjoint pressure is initially an adjoint sound wave, excited along

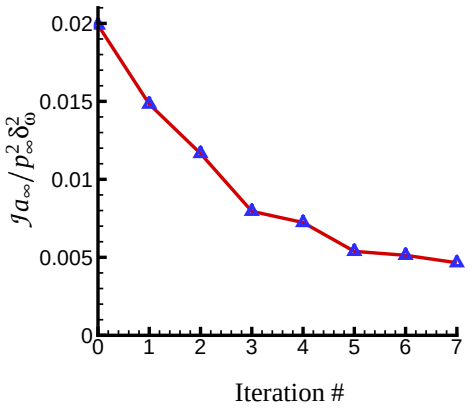

Fig. 4 The reduction of the cost.

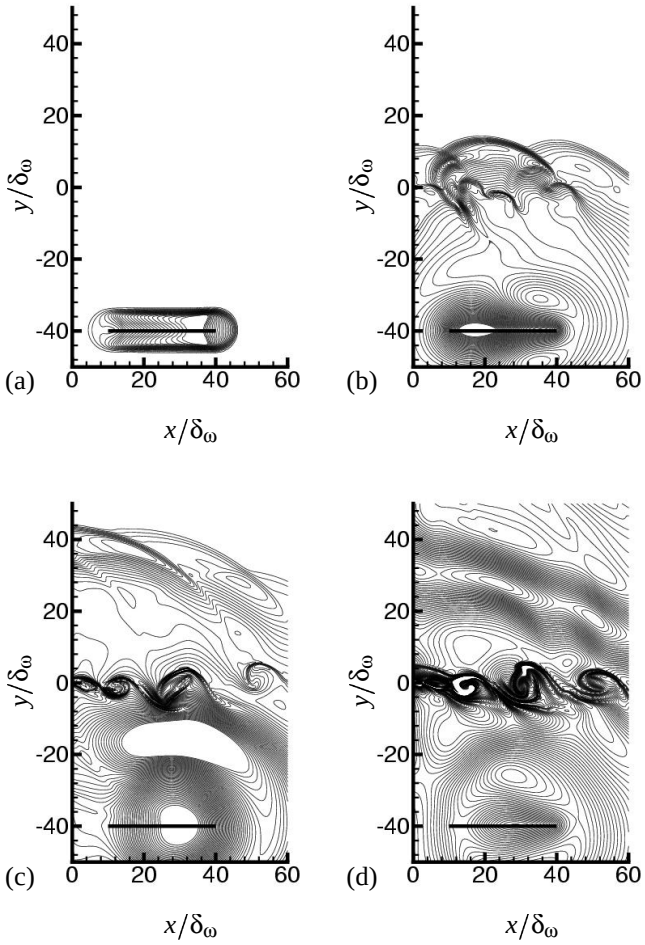

Fig. 5 Adjoint pressure: (a) $t = 195\delta_\omega/a_\infty$, (b) $t = 150\delta_\omega/a_\infty$, (c) $t = 120\delta_\omega/a_\infty$, (d) $t = 75\delta_\omega/a_\infty$. The time goes backward in the adjoint solution.

the target line by the cost. As this wave encounters the mixing layer, it excites instability waves, which move upstream in the mixing layer to the control region. Finally, the gradient information is recorded inside this region. It is the instability waves in the adjoint that dominates the gradient, which suggests that the control mechanism is via the instabilities in the mixing layer.

Given this qualitative behavior of the adjoint, the mechanism of noise control can be expressed as follows. The control interacts with the flow. This excitation alters (slightly, we shall see) the instabilities in the flow. The modified flow field is quieter. Works are ongoing to identify the precise mechanism quantitatively.

Control Forcing

Figure 6 shows twenty snapshots of the optimal control forcing at different times. In the control box, the forcing is distributed in a non-intuitive manner. The apparent "structure" in the control $\phi(x,y)$ moves at a speed between $0.7U_c$ and $1.7U_c$, where U_c is the anticipated structure convection velocity. which is close to the expected convective speed U_c, but little else can be understood via visualizations.

In an attempt to develop a quantitative description of the action of the forcing, we define integrals over the control region to study the net influence on the flow:

$$Q(t) = \int_C q(\mathbf{x},t)\,dC. \tag{7}$$

Figure 7 shows the history of the net energy, velocity and control forcing in the control region. We see no correlation between the forcing and integrated flow variables in the control region. We anticipate that there must be some correlation, but more data will be needed to study its statistics if it is at all possible. The flat part at the end of the forcing history is caused by the time delay between the control and the target. Control in that flat piece would not alter $\mathcal{J}$ on the target line in $t_0 < t < t_1$.

Flow Field Change

Despite the large decrease in the radiated sound, the mixing layer flow is changed surprising little by the control. Figure 8 shows the spreading of the mixing layer in terms of its momentum thickness,

$$\delta_m = \int_{-\infty}^{+\infty} \frac{\rho(u-U_1)(U_2-u)}{\rho_\infty \Delta U^2}\,dy. \tag{8}$$

We see that the control changes its downstream evolution only slightly. The waviness of the profiles is believed to be due to the limited statistical sample in the t_0 to t_1 simulation time, but might also be due to the nature of the parings which is known to cause jumps in thickness.

The turbulence kinetic energy, defined as

$$k = \frac{1}{2}\overline{\rho[(u')^2 + (v')^2]}, \tag{9}$$

where u' and v' are fluctuation of velocities, is also nearly unchanged. Figure 9 shows

$$K_x(x) = \int_{-50\delta_\omega}^{50\delta_\omega} k\,dy \tag{10}$$

and

$$K_y(y) = \int_0^{60\delta_\omega} k\,dx \tag{11}$$

with and without control. The noise reduction is clearly not due to turbulence suppression. Previously,[9] we also show that there is little change in how the energy is arranged in large turbulent structures. Only a slight change in their phasing was observed.

Conclusion

An adjoint-based approach has been developed that reduces the noise radiated by a two-dimensional mixing layer by 6.3dB along a specified line in the far-field.

The changes of the flow field due to the control forcing are relatively minor, which is possible because only a small fraction of the flow's energy, that with a supersonic phase velocity, radiates. Our simulations indicate that, at least in a two-dimensional mixing layer, this part can be altered with minimal control authority to dramatically reduce the noise.

The control forcing itself is non-intuitive and the correlations between it and other flow properties are not clear yet. Work continues identifying practical control laws and understanding the details of how the present control works.

Acknowledgment

We gratefully acknowledge the financial support of AFOSR and the computer resources provided by NPACI and NCSA.

References

[1]Lighthill, M. J., "On sound generated aerodynamically: I. General theory," *Proc. Royal Soc. Lond. A*, Vol. 211, 1952, pp. 564–587.

[2]Colonius, T., Lele, S. K., and Moin, P., "Sound generation in a mixing layer," *J. Fluid Mech.*, Vol. 330, 1997, pp. 375–409.

[3]Mitchell, B. E., Lele, S. K., and Moin, P., "Direct computation of the sound generated by vortex pairing in an axisymmetric jet," *J. Fluid Mech.*, Vol. 383, 1999, pp. 113–142.

[4]Freund, J. B., Lele, S. K., and Moin, P., "Direct numerical simulation of a Mach 1.92 turbulent jet and its sound field," *AIAA J.*, Vol. 38, No. 11, 2000, pp. 2023–2031.

[5]Freund, J. B., "Noise sources in a low-Reynolds-number turbulent jet at Mach 0.9," *J. Fluid Mech.*, Vol. 438, 2001, pp. 277–305.

[6]Lilley, G. M., "Jet Noise: Classical theory and experiments," In *Aeroacoustics of Flight Vehicles* edited by H. Hubbard. NASA RP 1258, 1991.

[7]Saiyed, N. H., Mikkelsen, K. L., and Bridges, J. E., "Acoustics and thrust of separate flow exhaust nozzles with mixing devices investigated for high bypass ratio engines," 6th AIAA/CEAS Aeroacoustics Conference, Lahaina, AIAA Paper 2000-1961, 2000.

[8]"Separate Flow Low Noise Nozzle Project," Nasa Aerospace Technology News, Volume 1, Issue 2, September 2000.

[9]Wei, M. and Freund, J. B., "Optimal control of free shear flow noise," 40th Aerospace Sciences Meeting, Reno, NV, AIAA Paper 2002-0665, January 2002.

[10]Bewley, T. R., Moin, P., and Temam, R., "DNS-based predictive control of turbulence: an optimal benchmark for feedback algorithms," *J. Fluid Mech.*, Vol. 477, 2001, pp. 179–225.

[11]Press, W. H., Flannery, B. P., Teukolsky, S. A., and Vetterling, W. T., *Numerical Recipes*, Cambridge, 1986.

[12]Lele, S. K., "Compact finite difference schemes with spectral-like resolution," *J. Comp. Phys.*, Vol. 103, 1992, pp. 16–42.

[13]Tam, C. K. W. and Webb, J. C., "Dispersion-relation-preserving finite difference schemes for computational acoustics," *J. Comp. Phys.*, Vol. 107, No. 2, Aug 1993, pp. 262–281.

[14]Freund, J. B., "A proposed inflow/outflow boundary condition for direct computation of aerodynamic sound," *AIAA J.*, Vol. 35, No. 4, 1997, pp. 740–742.

[15]Giles, M. B., "Nonreflecting boundary conditions for Euler equations calculations," *AIAA J.*, Vol. 18, 1990, pp. 2050–2058.

[16]Monkewitz, P. A. and Huerre, P., "Influence of the velocity ratio on the spatial instabilty of mixing layers," *Phys. Fluids*, Vol. 25, 1988, pp. 1137–1143.

[17]Ho, C. M. and Huerre, P., "Perturbed free shear layers," *Ann. Rev. Fluid Mech.*, Vol. 16, 1984, pp. 365–424.

[18]Sandham, N. and Reynolds, W., "Three-dimensional simulations of large eddies in the compressible mixing layer," *J. Fluid Mech.*, Vol. 224, 1991, pp. 133–158.

[19]Day, M. J., Reynolds, W. C., and Mansour, N. N., "The structure of the compressible reacting mixing layer: Insights from linear stability analysis," *Phys. Fluids*, Vol. 10, 1998, pp. 993–1007.

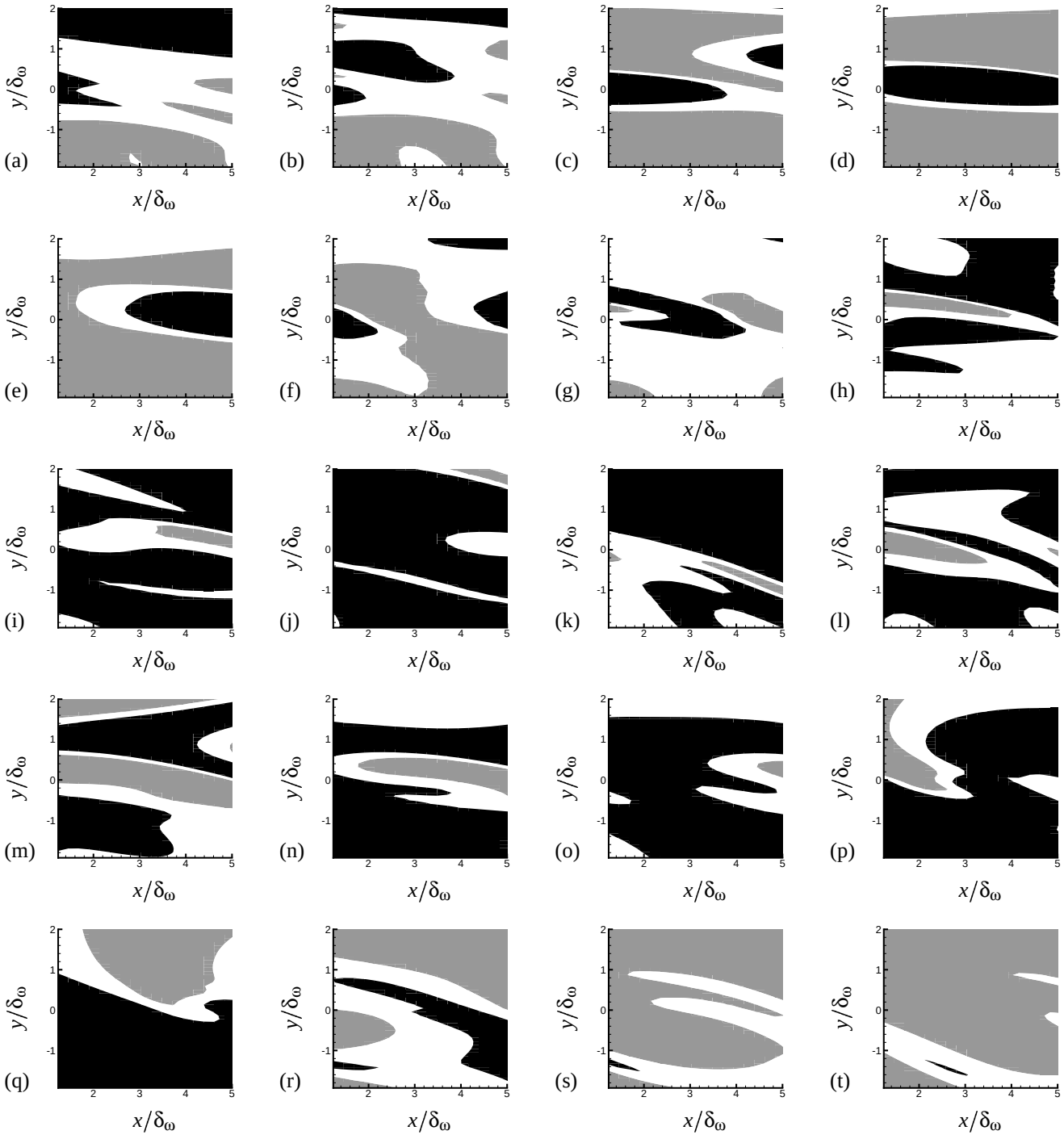

Fig. 6 Control forcing: (a) $t = 0$**, (b)** $t = 5\delta_\omega/a_\infty$**, (c)** $t = 10\delta_\omega/a_\infty$**, (d)** $t = 15\delta_\omega/a_\infty$**, (e)** $t = 20\delta_\omega/a_\infty$**, (f)** $t = 25\delta_\omega/a_\infty$**, (g)** $t = 30\delta_\omega/a_\infty$**, (h)** $t = 35\delta_\omega/a_\infty$**, (i)** $t = 40\delta_\omega/a_\infty$**, (j)** $t = 45\delta_\omega/a_\infty$**, (k)** $t = 50\delta_\omega/a_\infty$**, (l)** $t = 55\delta_\omega/a_\infty$**, (m)** $t = 60\delta_\omega/a_\infty$**, (n)** $t = 65\delta_\omega/a_\infty$**, (o)** $t = 70\delta_\omega/a_\infty$**, (p)** $t = 75\delta_\omega/a_\infty$**, (q)** $t = 80\delta_\omega/a_\infty$**, (r)** $t = 85\delta_\omega/a_\infty$**, (s)** $t = 90\delta_\omega/a_\infty$**, (t)** $t = 95\delta_\omega/a_\infty$**. Black indicates the positive forcing (**$> 0.01\rho_\infty a_\infty^3/\delta_\omega$**), and gray indicates the negative forcing (**$< 0.01\rho_\infty a_\infty^3/\delta_\omega$**).**

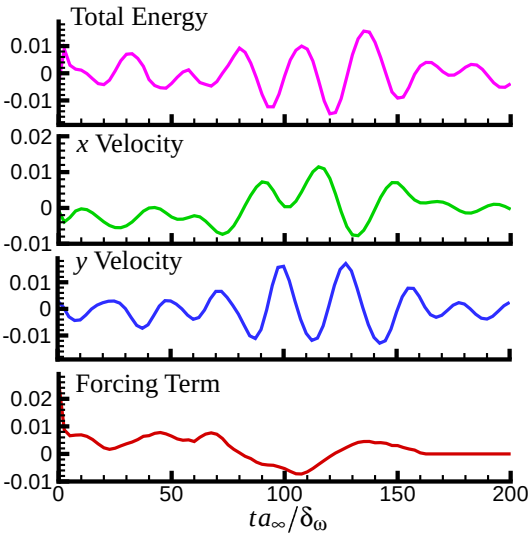

Fig. 7 History of integrals inside the control region.

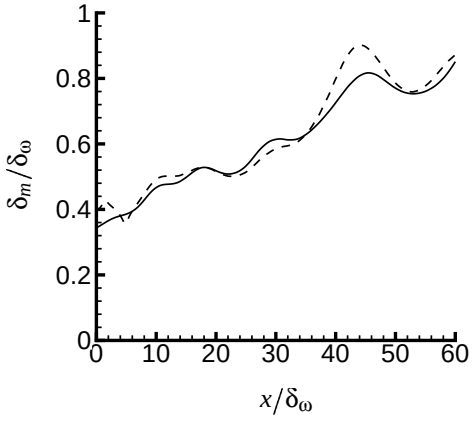

Fig. 8 Change of the momentum thickness of the mean flow: ——— without control; – – – – with control.

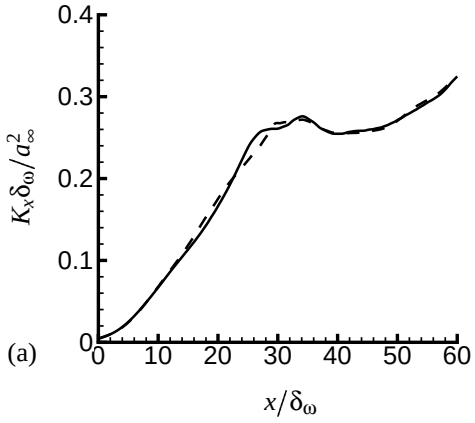

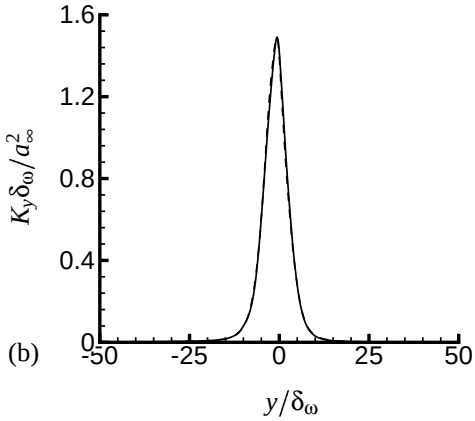

Fig. 9 Comparison of integrated turbulence kinetic energy as defined in (a) equation (10) and (b) equation (11). The lines indicate the case without control ——— and the case with control – – – – .